ChemComm

COMMUNICATION

View Article Online
View Journal | View Issue

Cite this: *Chem. Commun.*, 2022, **58**, 3701

Received 15th February 2022,
Accepted 21st February 2022

DOI: 10.1039/d2cc00680d

rsc.li/chemcomm

The overlooked NIR luminescence of $Cr(ppy)_3$†

Laura Stein,[a] Pit Boden,[b] Robert Naumann,[a] Christoph Förster,[a] Gereon Niedner-Schatteburg[b] and Katja Heinze*[a]

$Cr(ppy)_3$, a structural analog of the green phosphorescent $Ir(ppy)_3$, emits even in solution at room temperature from a weakly distorted spin–flip state at 910 nm (Hppy = 2-phenylpyridine). The low energy arises from an enhanced covalence of the Cr–C bonds as compared to Cr–N bonds. Lower temperature reduces thermally activated decay increasing the emission intensity.

Cyclometalated complexes, in particular of d^6 metal ions such as Ru^{II},[1,2] Ir^{III}[3,4] or Fe^{II}[5–7] possessing intense metal-to-ligand charge transfer (MLCT) absorptions, have shaped the field of organometallic photochemistry. The prototypical complex *fac*-$Ir(ppy)_3$ (Hppy = 2-phenylpyridine)[8,9] with its intense green ^{3}MLCT luminescence has paved the way to efficient luminescent materials for PHOLED applications,[10,11] while cyclometalated Ru^{II} complexes are less luminescent.[1,2] The first reported cyclometalated Fe^{II} counterparts are even non-luminescent[5,6] and a phosphorescent iron(II) complex was reported only recently.[7] In all d^6 cases, $^{1/3}$MLCT states play key roles for absorption and emission, while highly distorted metal centered excited triplet/quintet states ($^{3/5}$MC) provide non-radiative decay pathways in Ru^{II} and Fe^{II} complexes, which hamper efficient ^{3}MLCT luminescence.[1,10] Novel developments in the field of Earth-abundant complex chromophores beyond precious metal phosphors led to a paradigm change.[12–16] Beside CT states, metal-centered spin–flip excited states can be highly luminescent between 709–775 nm as demonstrated with polypyridine Cr^{III} complexes.[17–22] A higher covalent bonding in a carbazolato pyridine Cr^{III} complex $[Cr(dpc)_2]^+$ (dpc = 3,6-di-*tert*-butyl-1,8-di(pyridine-2-yl)-carbazolato) shifted the emission to lower energy (λ_{em} = 1067 nm, 77 K). However, this went along with a poor quantum yield ($\Phi < 0.00089\%$).[23]

We investigate the effect of cyclometalation on the spin–flip emission of Cr^{III} reporting the structure and photophysical properties of $Cr(ppy)_3$ as a $3d^3$ structural analog of the $5d^6$ complex $Ir^{III}(ppy)_3$.[8,9] $Cr(ppy)_3$ was first prepared in 1967 by treating $CrCl_3$x3THF with 2-(*ortho*-lithiophenyl)pyridine[24] and later (1991) by treating $CrPh_3(thf)_3$[25] with 2-phenylpyridine.[26] Despite its existence for decades, neither the stereochemistry, nor emission properties of $Cr(ppy)_3$ were reported.[24,26]

Single crystals of the facial isomer *fac*-$Cr(ppy)_3$ suitable for X-ray diffraction (XRD) analysis were obtained after heating $CrPh_3(thf)_3$ with 2-phenylpyridine in THF and recrystallisation from CH_2Cl_2/toluene (Fig. 1). *fac*-$Cr(ppy)_3$ crystallised in the tetragonal space group $P\bar{4}2_1c$ as *fac*-$Ir(ppy)_3$ obtained from sublimation,[27] while $Ir(ppy)_3$ crystallised from solution as twinned crystals in the trigonal space group $P\bar{3}$, resulting in superimposed Ir-coordinated C/N positions.[28]

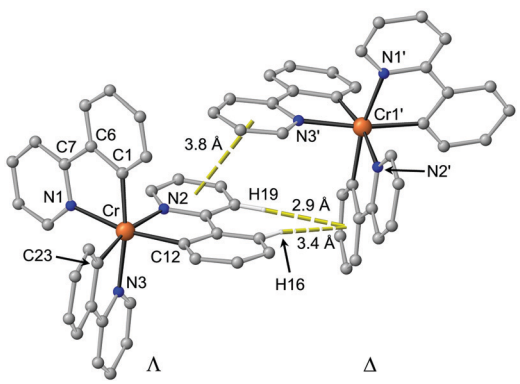

Fig. 1 Molecular structure of *fac*-$Cr(ppy)_3$ in the solid state with π···π and CH···π contacts between *Δ* and Λ isomers shown as yellow dashed lines. Hydrogen atoms (except those involved in CH···π contacts) are omitted for clarity. The π···π contact is denoted by the distance between ring centroids. CH···π contacts are denoted by the distance from the hydrogen atom to the ring centroid.

[a] *Johannes Gutenberg-University, Department of Chemistry, Duesbergweg 10-14, Mainz, Germany. E-mail: katja.heinze@uni-mainz.de; Tel: +49 6131 3925886*
[b] *Department of Chemistry and Research Center Optimas, TU Kaiserslautern, Erwin-Schrödinger-Straße 52, 67663 Kaiserslautern, Germany*

† Electronic supplementary information (ESI) available. CCDC 2124885. For ESI and crystallographic data in CIF or other electronic format see DOI: 10.1039/d2cc00680d

In the present XRD analysis, the C/N assignment and the facial configuration were confirmed by inspection of the thermal ellipsoids of the atoms of the alternative assignment and the resulting *R* factors. The Cr–C distances are shorter than the Cr–N distances (d_{av}(Cr–C) = 2.059(2) Å, d_{av}(Cr–N) = 2.145(2) Å; ESI,† Table S1 and Fig. S1). The Cr–N distances in $[Cr(bpy)_3][PF_6]_3$[29] (bpy = 2,2′-bipyridine; *d*(Cr–N) = 2.042(5) Å) are significantly smaller, substantiating a trans influence of the carbon donor in *fac*-Cr(ppy)$_3$. Quantum chemical calculations yield *d*(Cr–C) = 2.063 Å and *d*(Cr–N) = 2.146 Å in very good agreement with the XRD data (ESI,† Table S1 and Fig. S1). The geometry of the $[CrC_3N_3]$ coordination sphere in *fac*-Cr(ppy)$_3$ is close to octahedral, similar to the $[CrN_6]$ coordination of $[Cr(bpy)_3]^{3+}$ (ESI,† Table S2). π···π and CH···π contacts are observed between Δ and Λ isomers in the solid state of *fac*-Cr(ppy)$_3$ (Fig. 1), while no such contacts appear in the salt $[Cr(bpy)_3][PF_6]_3$.[29] Analytical data of *fac*-Cr(ppy)$_3$ are compiled in the ESI† (Fig. S3 and S4).

While polypyridine Cr^{III} complexes are reduced either at the ligand to give radical anions or at the metal center to give Cr^{II},[17,20,22,30,31] *fac*-Cr(ppy)$_3$ is not reduced up to potentials of −2.2 V *vs.* ferrocene (ESI,† Fig. S3), likely due to the electron-rich ppy^- ligand. An irreversible oxidation is observed at a peak potential E_p = +0.24 V *vs.* ferrocene, which is assigned to an oxidation of the Cr-aryl moiety with a covalent Cr–C bond.

The optical properties of *fac*-Cr(ppy)$_3$ were probed in solution and in the solid state (ESI,† Fig. S5–S10). The absorption band at 440 nm (ε = 3000 M^{-1} cm^{-1} in CH_2Cl_2, Fig. 2a) and around 450 nm in a KBr pellet (ESI,† Fig. S7) is assigned to transitions with ILCT/MLCT character (calcd. at 414 nm, *f* = 0.0016 (E); 409 nm, *f* = 0.0041 (A)) according to time-dependent DFT calculations and CT number analyses (Fig. 2a; ESI,† Fig. S2).[32,33] The energetically next higher absorption band possesses a larger MLCT character (calcd. at 395 nm, *f* = 0.0294 (E); 387 nm, *f* = 0.0016 (A)) while the largely metal centered $^4T_2$ states are calculated at 350/348 nm (*f* = 0.0108/0.0025 (A/E)). The MLCT bands are responsible for the yellow-orange colour of the complex (Fig. 2b, inset). Excited states with MLCT/ILCT character are compatible with the oxidation of *fac*-Cr(ppy)$_3$ at E_p = 0.24 V and the reduction below −2.2 V *vs.* ferrocene (ESI,† Fig. S3), similar to the redox processes assigned for *fac*-Ir(ppy)$_3$ at 0.31 and −2.7 V in DMF.[34]

Excitation of *fac*-Cr(ppy)$_3$ dissolved in deaerated 2-MeTHF or CH_2Cl_2 at 293 K results in sharp emission bands peaking at 910 nm with $FWHM_{293K}$ ≈ 1185/1068 cm^{-1}, respectively (Fig. 2b; ESI,† Fig. S5). The band shifts to 890 nm and sharpens to $FWHM_{77K}$ ≈ 540 cm^{-1} at 77 K in frozen 2-MeTHF, revealing some fine structure (890, 910 (sh), 1020 (sh) nm). The integrated emission intensity increases *ca.* fivefold (Fig. 2b). The excitation spectra at 298 and 77 K in 2-MeTHF solution follow the absorption spectrum (ESI,† Fig. S6). This confirms that the emission arises from initially excited ILCT/MLCT states (350–500 nm) of *fac*-Cr(ppy)$_3$, which efficiently evolve to the emissive state in 2-MeTHF (ESI,† Fig. S6a). This also holds for excitation and emission properties in CH_2Cl_2 at 293 K (ESI,† Fig. S5 and S6b) and in the solid state (ESI,† Fig. S7). The luminescence lifetimes at 293 and 77 K in 2-MeTHF amount to 9.5 and 48 μs, respectively and to 9.3 μs in CH_2Cl_2 at 293 K (ESI,† Fig. S8 and S9). In the powder the decay is biexponential with 10 μs (76%) and 3 μs (24%) (ESI,† Fig. S10), possibly due to energy migration in the solid *via* the π···π and CH···π contacts (Fig. 1) as has been observed *e.g.* for Ir(ppy)$_3$.[35,36]

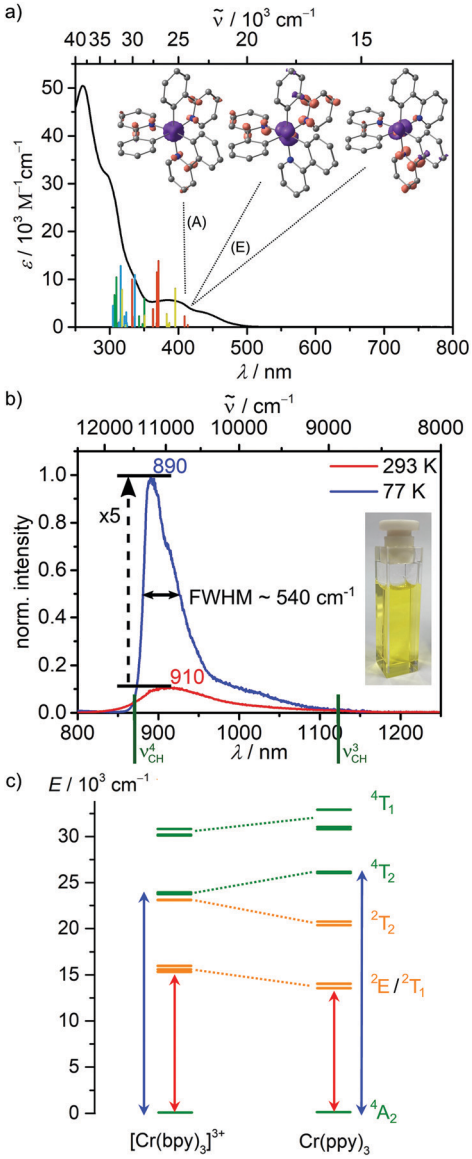

Fig. 2 (a) UV/Vis absorption spectrum of *fac*-Cr(ppy)$_3$ (black) in CH_2Cl_2 at 293 K including TD-DFT calculated transitions. The code indicates the character of the transition according to CT number analysis (green: MC, red: ILCT yellow: MLCT, orange: LMCT, blue: LLCT) and difference densities of the three lowest energy transitions (E and A, isosurface at 0.005 a.u., purple = electron depletion, orange = electron gain). (b) Emission spectra of *fac*-Cr(ppy)$_3$ in 2-MeTHF at 293 K (red) and 77 K (blue) (λ_{exc} = 420 nm) with the energies of CH overtones[19] ν^3 and ν^4 indicated in green and a photograph of *fac*-Cr(ppy)$_3$ in 2-MeTHF (inset). (c) Quartet (green) and doublet (orange) energy levels of $[Cr(bpy)^{3]3+}$ and *fac*-Cr(ppy)$_3$ from CASSCF(7,12)-NEVPT2 calculations showing the increased ligand field splitting (blue arrows) and decreased spin–flip state energy (red arrows) for *fac*-Cr(ppy)$_3$ (labels according to octahedral symmetry, although the actual symmetry is lower).

Nanosecond laser flash photolysis experiments of *fac*-$Cr(ppy)_3$ in Ar-saturated CH_2Cl_2 yielded a transient absorption (TA) spectrum with excited state absorptions (ESA) throughout the visible region, superimposed to the ground state bleach below 500 nm (ESI,† Fig. S11). The TA spectrum of *fac*-$Cr(ppy)_3$ differs from reported TA spectra of pyridine and acetylacetonato Cr^{III} complexes displaying only a single ESA around 520–540 nm.[22,37–40] The apparent ESA bands at 485 nm and 640 nm decay monoexponentially with τ = 10.2 μs and 9.9 μs, respectively (ESI,† Fig. S11 and S12), in agreement with the luminescence decay.

Compared to $[Cr(bpy)_3]^{3+}$ (λ_{em} = 729 nm, HCl_{aq}),[41] the spin–flip emission band of *fac*-$Cr(ppy)_3$ is bathochromically shifted by ≈ 2730 cm^{-1}. CASSCF(7,12)-NEVPT2 calculations on geometry-optimised $[Cr(bpy)_3]^{3+}$ and *fac*-$Cr(ppy)_3$ complexes correctly predict the bathochromic shift of the spin–flip luminescence (1773 cm^{-1}; Fig. 2c; ESI,† Table S5). With respect to the carbazolato pyridine Cr^{III} complex $[Cr(dpc)_2]^{+}$[23] the luminescence band of *fac*-$Cr(ppy)_3$ appears at higher energy by ≈ 1860 cm^{-1} (77 K). Obviously, the combination of σ/π-donating carbanionic donors and π-accepting pyridines along all axes *x*, *y* and *z* in *fac*-$Cr(ppy)_3$, achieves a metal–ligand bond covalence in-between that of $[Cr(bpy)_3]^{3+}$[41] and $[Cr(dpc)_2]^{+}$.[23]

Contrary to $[Cr(dpc)_2]^{+}$ emitting only at 77 K,[23] *fac*-$Cr(ppy)_3$ emits at 293 K in fluid 2-MeTHF or CH_2Cl_2 (Φ = 0.03% in CH_2Cl_2; Φ = 0.02% as powder). Although these quantum yields are still below the record values of molecular rubies of up to Φ = 20% in solution,[17–22] this marks a great advancement for open-shell complexes made from abundant transition metals emitting in the NIR region above 800 nm in fluid solution.

As the quantum yields increase at lower temperature, a thermally activated decay pathway is likely operative.[41] For the tris(bidentate) Cr^{III} complex $[Cr(bpy)_3]^{3+}$ (Φ = 0.25 ± 0.02%, τ = 69 ± 2 μs in 1 M HCl at 296–297 K) an activation barrier for thermal non-radiative deactivation of 43 ± 1 kJ mol^{-1} has been determined.[41] A thermally activated trigonal twist has been suggested as possible non-radiative pathway for tris(bidentate) quasi-cage Cr^{III} complexes.[42] Compared to the rather flexible bpy ligand in $[Cr(bpy)_3]^{3+}$, the more rigid 1,10-phenanthroline ligand phen endows a higher Φ and τ in $[Cr(phen)_3]^{3+}$ (Φ = 1.2 ± 0.1%, τ = 304 ± 4 μs in 1 M HCl at 296–297 K).[41] Therefore, trigonal twisting and intraligand torsional modes might be operating in the excited *fac*-$Cr(ppy)_3$ complex as well, leading to thermally activated surface crossing. This implies that the relaxed excited doublet state is distorted relative to the ground state (see below).

Non-radiative multiphonon relaxation, *i.e.* electronic to vibrational energy transfer to overtones of high-energy oscillators, such as C–H modes, might not be very important for *fac*-$Cr(ppy)_3$ as the relevant overtones determined from a model ligand (Me_2-bpy; ν^3 = 8792 cm^{-1} (1137 nm) and ν^4 = 11493 cm^{-1} (870 nm))[19] possess only a small spectral overlap with the emission band of *fac*-$Cr(ppy)_3$ at 910 nm (Fig. 2b). A further non-radiative pathway involving back-intersystem crossing to the metal centered quartet states appears unlikely as well, considering the strongfield ligand ppy^{-}. TDDFT and CASSCF(7,12)-NEVPT2 calculations suggest an even larger ligand field splitting (energy difference between $^4T_2$ and $^4A_2$ states) in *fac*-$Cr(ppy)_3$ than in $[Cr(bpy)_3]^{3+}$ (by 2285 cm^{-1}; Fig. 2c). Finally, energy transfer between uncharged *fac*-$Cr(ppy)_3$ complexes in solution and in the solid is a possible self-quenching pathway mediated by π···π and CH···π contacts (Fig. 1), while self-quenching of charged Cr^{III} complexes requires high chloride concentrations to form ion clusters in solution.[43,44]

To obtain information on the potential distortion of the excited doublet state, step-scan FTIR spectra of *fac*-$Cr(ppy)_3$ were collected (KBr pellet, λ_{exc} = 355 nm, 20 K). The spectra display ESA and bleaching bands (ESI,† Fig. S13a). The excited state FTIR spectrum consequently differs from the ground state spectrum (ESI,† Fig. S13b), confirming that the long-lived doublet state is distorted with respect to the ground state. At 20 K in KBr, this doublet state decays monoexponentially with τ = 9.8 μs, as derived from a global fit of decay traces at 1286, 1397, 1442, 1461 and 1475 cm^{-1} (ESI,† Fig. S14 and Table S3). DFT geometry optimisations and frequency analyses (ESI,† Fig. S15 and S16) substantiate that the lowest energy doublet state is indeed distorted relative to the quartet ground state: Cr–C and Cr–N distances change from 2.063 Å to 2.044, 2.053 and 2.055 Å and from 2.146 Å to 2.138, 2.147, 2.153 Å, respectively, while the X–Cr–Y angles remain rather constant (ESI,† Fig. S17 and Table S1). In agreement with the experimentally obtained data, the DFT calculated vibrational frequencies for the quartet ground and the excited doublet state show similar shifts in energy (ESI,† Fig. S15 and S16, calculated frequencies scaled by 0.975).

The NIR luminescence of *fac*-$Cr(ppy)_3$ recorded in a KBr pellet between 290–5 K strongly increases below 100 K (ESI,† Fig. S18). While in solution the emission intensity increases *ca.* fivefold already at 77 K (Fig. 2b), the gain in intensity of the KBr pellet starts below *ca.* 80 K. This is compatible with a distorted excited state, which decays by thermal activation to the ground state. While the energy barriers appear higher in rigid matrices thanks to less distorted and hence more nested excited states the temperature dependence in frozen 2-MeTHF and KBr matrices is different (Fig. 2b, ESI,† Fig. S18).

Complexes *cis*-$[Cr(bpy)_2(Ar)_2]^{+}$ reductively eliminate Ar–Ar under irradiation,[45] while *fac*-$Cr(ppy)_3$ is photostable in 2-MeTHF (λ_{exc} = 420 nm, ESI,† Fig. S19) thanks to the absence of *cis*-positioned Ar ligands. Similarly, *trans*-[Cr(cyclam)$(C{\equiv}C{-}C_6H_4R)_2]^{+}$ appear to be photostable.[46] In CH_2Cl_2, some photoreactivity is observed for *fac*-$Cr(ppy)_3$ (ESI,† Fig. S20). Rather than photoreduction of CH_2Cl_2 itself (E = −2.6 V)[47] by the excited complex (E(*$Cr(ppy)_3$/$[Cr(ppy)_3]^{+}$) = −1.12 V), which is thermodynamically unfavourable, traces of HCl in the CH_2Cl_2 could lead to irreversible photooxidation of *$Cr(ppy)_3$ (ESI,† Fig. S3) and H^{+} reduction. Photo- and redox stable cyclometalated Cr^{III} complexes might by developed into useful photoreductants in the future.

fac-$Cr(ppy)_3$ is the first Cr^{III} spin–flip emitter with emission above 900 nm in solution at 293 K. The effect of carbanionic donors in place of pyridine donors is two-fold, namely the increase in energy of the metal centred quartet states, owing to

the larger ligand field strength, and the decrease of the energy of the spin–flip states, owing to the stronger Cr–C bond covalence (nephelauxetic effect). These insights on the photophysics of the cyclometalated Cr^{III} complex *fac*-Cr(ppy)$_3$ are complementary to recent discoveries for first row transition metal CT emitters[7,48–54] and demonstrate that fundamental ground-breaking studies can pave the way to fully exploiting Earth-abundant metals, *e.g.* in light harvesting, sensing, photocatalysis and optical devices.

K. H. designed the project and wrote the paper, L. S. and R. N. performed synthesis, characterization and DFT, P. B. and G. N. S. step-scan FTIR spectroscopy and luminescence in KBr.

Support from the Deutsche Forschungsgemeinschaft [SPP 2102 ''Light-controlled reactivity of metal complexes'' GE 961/10-01; HE 2778/10-2 and INST 247/1018-1] is gratefully acknowledged. Parts of this research used the supercomputer Elwetritsch and advisory services offered by TU Kaiserslautern (https://elwe.rhrk.uni-kl.de). We thank Dr. Luca M. Carrella for XRD data collection and Prof. Dr. Christoph Kerzig and Maria-Sophie Bertrams for TA support and usage authorisation.

Conflicts of interest

There are no conflicts to declare.

Notes and references

1 C. Kreitner and K. Heinze, *Dalton Trans.*, 2016, **45**, 13631.
2 T. C. Motley, L. Troian-Gautier, M. K. Brennaman and G. J. Meyer, *Inorg. Chem.*, 2017, **56**, 13579.
3 C. E. Housecroft and E. C. Constable, *Coord. Chem. Rev.*, 2017, **350**, 155.
4 A. R. B. M. Yusoff, A. J. Huckaba and M. K. Nazeeruddin, *Top. Curr. Chem.*, 2017, **375**, 39.
5 J. Steube, L. Burkhardt, A. Päpcke, J. Moll, P. Zimmer, R. Schoch, C. Wölper, K. Heinze, S. Lochbrunner and M. Bauer, *Chem. – Eur. J.*, 2019, **25**, 11826.
6 Z. Tang, X.-Y. Chang, Q. Wan, J. Wang, C. Ma, K.-C. Law, Y. Liu and C.-M. Che, *Organometallics*, 2020, **39**, 2791.
7 W. Leis, M. A. Argüello Cordero, S. Lochbrunner, H. Schubert and A. Berkefeld, *J. Am. Chem. Soc.*, 2022, **144**, 1169.
8 K. A. King, P. J. Spellane and R. J. Watts, *J. Am. Chem. Soc.*, 1985, **107**, 1431.
9 T. Hofbeck and H. Yersin, *Inorg. Chem.*, 2010, **49**, 9290.
10 M. A. Baldo, S. Lamansky, P. E. Burrows, M. E. Thompson and S. R. Forrest, *Appl. Phys. Lett.*, 1999, **75**, 4.
11 C. Adachi, M. A. Baldo, S. R. Forrest and M. E. Thompson, *Appl. Phys. Lett.*, 2000, **77**, 904.
12 C. Förster and K. Heinze, *Chem. Soc. Rev.*, 2020, **49**, 1057.
13 O. S. Wenger, *J. Am. Chem. Soc.*, 2018, **140**(42), 13522.
14 C. Bizzarri, E. Spuling, D. M. Knoll, D. Volz and S. Bräse, *Coord. Chem. Rev.*, 2018, **373**, 49.
15 B. M. Hockin, C. Li, N. Robertson and E. Zysman-Colman, *Catal. Sci. Technol.*, 2019, **9**, 889.
16 O. S. Wenger, *Chem. – Eur. J.*, 2019, **25**, 6043.
17 S. Otto, M. Grabolle, C. Förster, C. Kreitner, U. Resch-Genger and K. Heinze, *Angew. Chem., Int. Ed.*, 2015, **54**, 11572.
18 S. Otto, C. Förster, C. Wang, U. Resch-Genger and K. Heinze, *Chem. – Eur. J.*, 2018, **24**, 12555.
19 C. Wang, S. Otto, M. Dorn, E. Kreidt, J. Lebon, L. Sršan, P. Di Martino-Fumo, M. Gerhards, U. Resch-Genger, M. Seitz and K. Heinze, *Angew. Chem., Int. Ed.*, 2018, **57**, 1112.
20 S. Treiling, C. Wang, C. Förster, F. Reichenauer, J. Kalmbach, P. Boden, J. P. Harris, L. Carrella, E. Rentschler, U. Resch-Genger, C. Reber, M. Seitz, M. Gerhards and K. Heinze, *Angew. Chem., Int. Ed.*, 2019, **58**, 18075.
21 J.-R. Jiménez, B. Doistau, C. M. Cruz, C. Besnard, J. M. Cuerva, A. G. Campaña and C. Piguet, *J. Am. Chem. Soc.*, 2019, **141**, 13244.
22 F. Reichenauer, C. Wang, C. Förster, P. Boden, N. Ugur, R. Báez-Cruz, J. Kalmbach, L. M. Carrella, E. Rentschler, C. Ramanan, G. Niedner-Schatteburg, M. Gerhards, M. Seitz, U. Resch-Genger and K. Heinze, *J. Am. Chem. Soc.*, 2021, **143**, 11843.
23 N. Sinha, J.-R. Jiménez, B. Pfund, A. Prescimone, C. Piguet and O. S. Wenger, *Angew. Chem., Int. Ed.*, 2021, **60**, 23722.
24 K. Madeja, E. Hüsing and N. Ahrens, *Z. Chem.*, 1967, **7**, 22.
25 W. Herwig and H. Zeiss, *J. Am. Chem. Soc.*, 1959, **81**, 4798.
26 H. Drevs, *Z. Anorg. Allg. Chem.*, 1991, **605**, 145.
27 R. J. F. Berger, H.-G. Stammler, B. Neumann and N. W. Mitzel, *Eur. J. Inorg. Chem.*, 2010, 1613.
28 J. Breu, P. Stössel, S. Schrader, A. Starukhin, W. J. Finkenzeller and H. Yersin, *Chem. Mater.*, 2005, **17**, 1745.
29 K. V. Goodwin, W. T. Pennington and J. D. Petersen, *Inorg. Chem.*, 1989, **28**, 2016.
30 C. C. Scarborough, S. Sproules, T. Weyhermüller, S. DeBeer and K. Wieghardt, *Inorg. Chem.*, 2011, **50**, 12446.
31 P. M. Becker, C. Förster, L. M. Carrella, P. Boden, D. Hunger, J. van Slageren, M. Gerhards, E. Rentschler and K. Heinze, *Chem. – Eur. J.*, 2020, **26**, 7199.
32 F. Plasser, *J. Chem. Phys.*, 2020, **152**, 084108.
33 S. Mai, F. Plasser, J. Dorn, M. Fumanal, C. Daniel and L. González, *Coord. Chem. Rev.*, 2018, **361**, 74.
34 A. B. Tamayo, B. D. Alleyne, P. I. Djurovich, S. Lamansky, I. Tsyba, N. N. Ho, R. Bau and M. E. Thompson, *J. Am. Chem. Soc.*, 2003, **125**, 7377.
35 C. Tonnel, M. Stroet, B. Caron, A. J. Clulow, R. C. R. Nagiri, A. K. Malde, P. L. Burn, I. R. Gentle, A. E. Mark and B. J. Powell, *Angew. Chem., Int. Ed.*, 2017, **56**, 8402.
36 S. Sanderson, G. Vamvounis, A. E. Mark, P. L. Burn, R. D. White and B. W. Philippa, *J. Chem. Phys.*, 2021, **154**, 164101.
37 S. Otto, A. M. Nauth, E. Ermilov, N. Scholz, A. Friedrich, U. Resch-Genger, S. Lochbrunner, T. Opatz and K. Heinze, *ChemPhotoChem*, 2017, **1**, 344.
38 F. A. Baptista, D. Krizsan, M. Stitch, I. V. Sazanovich, I. P. Clark, M. Towrie, C. Long, L. Martinez-Fernandez, R. Improta, N. A. P. Kane-Maguire, J. M. Kelly and S. J. Quinn, *J. Am. Chem. Soc.*, 2021, **143**, 14766.
39 N. Serpone and M. Z. Hoffman, *J. Phys. Chem.*, 1987, **91**, 1737.
40 E. A. Juban and J. K. McCusker, *J. Am. Chem. Soc.*, 2005, **127**, 6857.
41 A. M. McDaniel, H.-W. Tseng, N. H. Damrauer and M. P. Shores, *Inorg. Chem.*, 2010, **49**, 7981.
42 M. W. Perkovic, M. J. Heeg and J. F. Endicott, *Inorg. Chem.*, 1991, **30**, 3140.
43 R. Sriram, M. Z. Hoffman, M. A. Jamieson and N. Serpone, *J. Am. Chem. Soc.*, 1980, **102**, 1754.
44 M. A. Jamieson, N. Serpone and M. Z. Hoffman, *Coord. Chem. Rev.*, 1981, **39**, 121.
45 B. E. Olafsen, G. V. Crescenzo, L. P. Moisey, B. O. Patrick and K. M. Smith, *Inorg. Chem.*, 2018, **57**, 9611.
46 D. L. Grisenti, W. W. Thomas, C. R. Turlington, M. D. Newsom, C. J. Priedemann, D. G. VanDerveer and P. S. Wagenknecht, *Inorg. Chem.*, 2008, **47**, 11452.
47 A. Kotsinaris, G. Kyriacou and C. Lambrou, *J. Appl. Electrochem.*, 1998, **28**, 613.
48 M. Dorn, J. Kalmbach, P. Boden, A. Päpcke, S. Gómez, C. Förster, F. Kuczelinis, L. M. Carrella, L. Büldt, N. Bings, E. Rentschler, S. Lochbrunner, L. González, M. Gerhards, M. Seitz and K. Heinze, *J. Am. Chem. Soc.*, 2020, **142**, 7947.
49 L. A. Büldt, X. Guo, R. Vogel, A. Prescimone and O. S. Wenger, *J. Am. Chem. Soc.*, 2017, **139**, 985.
50 P. Herr, C. Kerzig, C. B. Larsen, D. Häussinger and O. S. Wenger, *Nat. Chem.*, 2021, **13**, 956.
51 K. S. Kjær, N. Kaul, O. Prakash, P. Chábera, N. W. Rosemann, A. Honarfar, O. Gordivska, L. A. Fredin, K. E. Bergquist, L. Häggström, T. Ericsson, L. Lindh, A. Yartsev, S. Styring, P. Huang, J. Uhlig, J. Bendix, D. Strand, V. Sundström, P. Persson, R. Lomoth and K. Wärnmark, *Science*, 2019, **363**, 249.
52 A. K. Pal, C. F. Li, G. S. Hanan and E. Zysman-Colman, *Angew. Chem., Int. Ed.*, 2018, **57**, 8027.
53 M. Gernert, L. Balles-Wolf, F. Kerner, U. Müller, A. Schmiedel, M. Holzapfel, C. M. Marian, J. Pflaum, C. Lambert and A. Steffen, *J. Am. Chem. Soc.*, 2020, **142**, 8897.
54 B. Hupp, C. Schiller, C. Lenczyk, M. Stanoppi, K. Edkins, A. Lorbach and A. Steffen, *Inorg. Chem.*, 2017, **56**, 8996.

